




Research Article


Investigating the strength, hydraulic conductivity, and durability of the CSG (cemented sand-gravel) check dams: a case study in Iran



Hamed Farshbaf Aghajani¹  · Hossein Soltani-Jigheh¹ · Mohammad Salimi¹ · Sina Karimi¹ · Vahid Estekanchi¹ · Reza Akbarzadeh Ahari²

Received: 19 December 2021 / Accepted: 4 May 2022

Published online: 13 May 2022

© The Author(s) 2022 

Abstract

This paper aims to find a proper admixture of the cemented sand-gravel (CSG) material for constructing a hardfill embankment located in cold weather. To this end, the compaction, strength, permeability of the cemented sand-gravel mixtures with cement contents of 5, 7.5, 10, and 12.5% are experimentally studied. Besides, the freeze–thaw durability of native grains of the soil and stabilizing soil is examined. According to the test results, even though the compaction specifications of all mixtures do not considerably depend on the cement content, however the cement content in the mixture significantly influences the compressive strength, stiffness, and permeability of mixtures. The soil aggregates inherently have high water absorption and are thus severely fractured after 50 cycles of freeze–thaw. After stabilizing the soil grains with cement, the freeze–thaw durability of the cemented soil mixture is considerably improved, and the weight loss of all mixtures becomes less than 5% after 12 cycles of freeze–thaw. However, the freeze–thaw cycles reduce the mixture strength up to 40% in comparison with the intact mixture. The analysis of scanning electron microscope images implies that four factors including disintegration of the calcium-silicate-hydration complex, imposing new porosity, releasing interlayered water, and establishing the secondary ettringite are the main reasons for strength reduction of the cemented sand-gravel mixtures after encountering the freeze–thaw cycles which have not been observed in the previous researches.

Article Highlights

- The cemented sand gravel (CSG) mixture is an efficient and economical solution for the construction of sediment control check dams in cold regions.
- The durability of coarse-grained soils is improved after blending with a cementing agent.
- The freeze-thaw cycles alter the microstructure of the hardened cement paste within the CSG mixture and decrease the mixture strength.
- The durability, strength, and stiffness increase, and permeability decrease with increasing the cement content in the CSG mixture.

Keywords Cemented sand gravel (CSG) mixture · Freeze–thaw test · Compressive strength · Hardfill embankment · Check dam

✉ Hamed Farshbaf Aghajani, h.farshbaf@azaruniv.ac.ir | ¹Department of Civil Engineering, Faculty of Engineering, Azarbaijan Shahid Madani University, Kilometer 35 of Tabriz/Azarshahr Road, P.O. Box 53714-161, Tabriz, Iran. ²Department of Natural Resources and Watershed Management, East Azarbaijan Organization of Forests, Range and Watershed Management, Ministry of Agriculture-Jahad, 5157977391 Tabriz, Iran.



1 Introduction

The cemented sand-gravel mixture (CSG) is frequently used for constructing hardfill embankments. This type of material is prepared by mixing sand and gravel soils with a cementing agent in the presence of an adequate amount of moisture. The water content in the mixture is an essential element to complete the hydration process of the cement paste and facilitates the proper compaction of the mixture within the embankment [1]. From the strength aspect, the CSG material has greater strength and presents high cohesion due to the cementation action between grains. Therefore, hardfill embankments composed of CSG mixtures can be constructed with a steeper side slope and have a low volume in comparison with the conventional earthfill dams and embankments [2]. The first idea of a hardfill dam was proposed by Londe, Lino [3]. Since the last two decades, hardfill dams have been developed as a new solution for the construction of embankment dams concerning many advantages [2, 4]. Numerous hardfill dams were constructed in the world using CSG mixtures [1, 5, 6]. The cemented material dam (CMD) is the latest solution for hardfill dams, where the cement is blended with low-quality soil aggregates to produce the cemented material [7].

The appropriate participant of cement, soil aggregates, and water in CSG mixtures is determined based on achieving the desired strength, and maximum degree of compaction. However, in some regions encountering unusual environmental conditions such as cold weather, the durability of the CSG mixture under environmental effects may play an important role in the mixing design. One of the influencing factors is the durability of CSG mixtures under freeze–thaw cycles.

In the last decades, many researchers have focused on the behavior of stabilized clay subjected to freeze–thaw (F-T) and wetting–drying cycles [8–13]. The results of experimental investigations show some degradation in the shear strength and bearing capacity of fine-grained soils after subsequent F-T cycles [13–15]. Furthermore, the fissures and micro-cracks are the consequence of F-T that changes the structure of soils and influences the volume change and compressibility of soil [11, 13]. However, the strength and durability of stabilized soil are improved when the native soil is treated by mixing with some additives such as lime, cement, fly ash, fibers, and polymers. Shihata, Baghdadi [12] measured the compressive strength of treated soil after F-T cycles and showed a correlation between weight loss from the F-T test and uniaxial compressive strength (UCS), which can be used as a new means for evaluating the F-T resistance of a soil–cement mixture. Justin, Robert [9] concluded

that cement-treated soil has a weight loss of about 6% in the F-T cycles which is less than other stabilized soils treated with fly ash and lime agents. According to the test results of Ding et al. [8], the compressive strength of cement-treated soil sharply decreases after the first F-T cycle and then exhibits less reduction after the fifth cycle. Solanki et al. [16] concluded that a reduction in the compressive strength in the earlier cycles of F-T may be referred to as an increase in the moisture absorbed by the specimen during the thawing portion of the cycle. The results of a test conducted by Li et al. [15] indicated that whereas compressive strength of clay soil significantly decreased after the F-T cycles, adding cement to the clay soil led to an increase in the resistance of stabilized soil under the F-T cycles. Gao et al. [17] measured the statistic and dynamic strength of clay soil stabilized with basalt fiber reinforced cement in various F-T cycles. They showed that both UCS and dynamic strength of cemented soil decreased with F-T cycles in such a way that the 1st and 3rd cycles have the greatest impact on the strength reduction. Wu et al. [18] examined the F-T durability and UCS of a modified expansive soil with the cement and steel slag powder and concluded the volume change of the cemented soil specimens decreased after eight cycles of F-T. Moreover, the effect of F-T cycles on the durability and UCS decreased in the samples with greater curing time. Similar studies showed a positive effect of the cement on the reduction of the volume change in cement-treated expansive soil subjected to F-T cycles [19, 20].

Even though many experimental studies were conducted to investigate cement-treated clay soils under the F-T cycles, limited research [21] has been conducted for evaluating the cementation effect on the behavior of clean sand and gravel soils, especially in the frost condition. Jamshidi et al. [22] studied the effect of the F-T cycles on the permeability, microstructure, and dynamic response of silty sand soil stabilized with 10% cement and found that the permeability of cemented sand was doubled and considerable damage was imposed in the mixtures after the 7th cycle of F-T. Theivakularatnam, Gnanendran [23] conducted a vast experimental program for examining the durability of cemented granular soils under the F-T and wetting–drying cycles. In these tests, coarse-grained soil is mixed with the 1.5 and 3% of Portland cement-slag combination as the cementing agent. The test results showed the considerable effect of wetting–drying cycles on the destruction of cemented mixtures relative to the F-T cycles. Besides, the compressive strength of mixtures slightly increased after encountering 12 cycles of F-T, which was referred to as the reduction of moisture in the samples. Li et al. [24] prepared a mixture composed

of Aeolian sand and cement subjected to F-T cycles after two curing ages of 7 and 28 days. The cohesion of cemented mixtures decreased and friction angle increased by increasing the number of F-T cycles. Besides, the F-T cycles imposed three various patterns of cracks in the mixtures. Jamshidvand et al. [25] investigated the effect of F-T cycles on the microstructure and strength of cemented sand soil in which the base soil in the mixture contained various amounts of silt and different percentages of zeolite added to the cemented mixture. The uniaxial compressive strength and California bearing ratio (CBR) of all mixtures gradually decreased after the F-T cycles. However, adding zeolite to the cemented mixture presents a minimum reduction in strength due to F-T cycles. A similar trend was observed for the reduction of UCS with F-T cycles in the silty soil that was stabilized with cement in addition with the other reinforcement such as zeolite and fiber [26–30].

While the previous studies were focused on the individual specification of the cemented soils, few systematic investigations can be found that simultaneously investigate both key and durability specifications of the cemented sand-gravel content. However, construction of the hardfill dam in the cold region requires to investigate not only the strength and permeability but also the long-time durability of cemented sand-gravel mixture after encountering cold weather in a uniform framework which have not been studied in the previous studies. The northwest region of Iran has cold weather with below zero temperatures during most days of cold seasons and, in turn, the weather temperature rises to a high degree in the warm season of summer. Thus, the F-T cycles during the lifetime significantly impact the durability of the geotechnical structures such as embankments. This paper aims to study the key parameters and durability of

the cemented sand gravel (CSG) mixtures that are used for the construction of a sediment control check dam with a short height, which is categorized as a small dam. With this objective, a clean coarse-aggregate soil is blended with the various contents of Portland cement. Then, the topmost tests of the compaction, compressive strength, hydraulic conductivity are conducted on the mixtures with various cement contents, and the effect of cement content on the key parameters is determined. To examine the behavior of the CSG check dam in cold weather, the durability of individual grains and the CSG mixtures are tested in the F-T test. Besides, the effect of the F-T cycles on the strength and stiffness of the mixture is determined. To interpret the strength reduction trend of the mixture after encountering F-T cycles, the microstructure of a mixture with 10% cement is surveyed after some specific F-T cycles. The microstructure investigation of the cemented soil showed the alteration in the hydrated cement paste structure after various F-T cycles which is different from the observed trend in the previous studies.

2 Material specifications, mixing design, and testing program

The stiffness, strength, permeability, F-T durability specifications, and microstructure of the CSG mixtures are investigated here. The CSG mixture is used for constructing a small check dam (for sediment control) that is located in Marand city in the northwest of Iran (Fig. 1). The photo from the dam body during the construction stage is shown in Fig. 2.

The native soil in the mixture is retrieved from the river bed strata near the small check dam site (located at

Fig. 1 The location of the CSG check dam in the Marand city of Iran





Fig. 2 The CSG check dam in the Marand city of Iran during construction

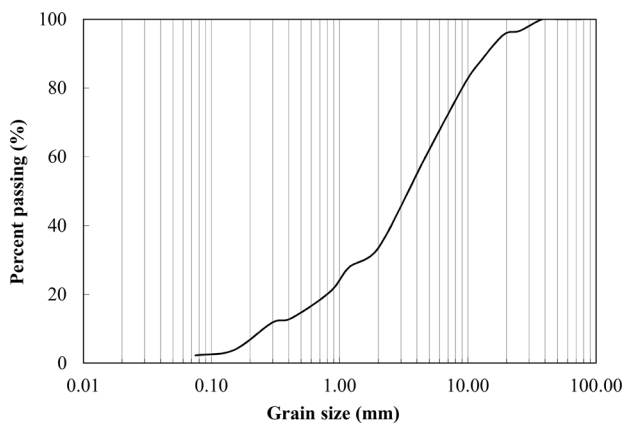


Fig. 3 The particle size distribution of soil fraction in the mixture

38.579043° N and 45.652973° E) and is composed of 40% sand and 58% gravel. The fine content of soil (passing through the No. 200 sieve) is about 2%. The particle size distribution of native soil is shown in Fig. 3. According to the unified soil classification system, the soil is categorized in the SW group. The maximum dry density (MDD) and optimum water content (OWC) of native soil are measured at 19.11 kN/m³ and 10.86%, respectively following the ASTM D698 [31].

The quality of grains was examined to implement the coarse-grained soil for producing the CSG mixture. The lists of key tests conducted on the CSG mixture and native soil are presented in Table 1. The degradation loss of material in the Los Angeles abrasion test [32] after 500 cycles is measured less than 30%. The weight loss of gravel and sand aggregates in the soundness sulfate sodium test is about 2% and 10%, respectively. Besides, other qualitative specifications of native soil such as

chemical components, needle and platy shape particles, clay lumps, friable particles, and organic impurities, lie in an acceptable range, and the native soil can be used as the aggregates in concrete from the aspect of aggregate quality.

Even though the satisfactory quality of soil grains, the results of apparent density [33, 34], oven-dried density, and water absorption tests (Table 2) indicate that solid grains of the native soil have a high degree of water absorption and low bulk density. The soil grains are originally formed by the destruction of the welded tuff bedrock, and the native soil is mainly composed of angular-shaped grains with intra-void porosity, which are seen in the scanning electron microscope (SEM) image of grains (Fig. 4). These porosity spaces cause high water absorption of the grains in order of 5%. Moreover, Marand city (the location of the CSG check dam) has cold weather in the winter and becomes warmer in summer, and the average long-term temperature of the city varies between – 12 °C in winter and 37 °C in summer. The high amount of water absorbed inside the grains may be frozen in winter and melted in the warm season. These frequent F-T cycles may break down and crush the grains. The result of the F-T test of aggregates conforms to the high susceptibility of grains to cracks in F-T cycles, which will be presented later.

The Portland type II cement is used as the cementation agent in the CSG mixture and has a Blaine value of 2974 (cm²/gr) and initial and final setting times of 116 and 175 min, respectively. The chemical composition of the cementing agent is presented in Table 3.

To select the best proportion of cement content within the CSG mixture, the native soil is blended with different cement contents of 5%, 7.5%, 10%, and 12.5%. The cement content corresponds to the weight ratio of dry cement to the dry weight of native soil fraction. In the first step, the key parameters of the CSG mixtures with different cement contents are determined and compared to determine the effect of cement content. These key parameters consist of the MDD and OWC relating to the compaction, stiffness and strength, strength evolution with curing time, and permeability. To this end, the compaction, uniaxial compressive strength, and permeability tests are conducted for all mixtures. Besides, the compaction and permeability of individual soil (without cementing agent) are determined and compared with the CSG mixtures. In the next step, the durability of the individual soil and stabilized soils with all ranges of cement contents are examined in sequence cycles of freeze–thaw. Besides, the strength of the mixture with 10% cement is measured after subjecting to the F-T cycles. To interpret the effect of the F-T cycles on the strength variation of the mixture after encountering F-T cycles, the microstructure of a mixture with 10% cement

Table 1 The list of the key tests conducted for the CSG mixtures and specimen specifications for each test

Test name	CSG mixture or native soil	Curing time (day)	Cement content in the mixture (%)	Specimen diameter (cm) or base dimension (in cm)	Specimen height (cm)	Test standard
Permeability (flexible wall chamber)	CSG mixture	14 and 28 days	5, 7.5, 10 and 12.5%	10	20	ASTM D5084 [37]
Permeability (rigid wall chamber)	Native soil	–	–	10	10.3	ASTM D5856 [43]
Uniaxial compression strength	CSG mixture	7 and 28 days	5, 7.5, 10 and 12.5%	15	30	ASTM D1633 [36]
Uniaxial compression strength after freeze–thaw cycles	CSG mixture	7 days	10% (four specimens)	15	30	ASTM D1633 [36]
Compaction	CSG mixture	Fresh state	5, 7.5, 10 and 12.5%	10.1	11.6	ASTM D558 [35]
Compaction	Native soil	–	–	10.1	11.6	ASTM D698 [31]
Freeze–thaw durability	CSG mixture	7 days	5, 7.5, 10 and 12.5%	Cubic (10 cm × 10 cm)	Cubic (10 cm)	ASTM D560 [38]
Freeze–thaw durability	Native soil	–	–			AASHTO T-103 [44]

Table 2 The apparent density, bulk density, SSD state density and water absorption of native soil aggregates (in accordance with ASTM C127 [33] and ASTM C128 [34])

Soil fraction	Apparent density (kN/m ³)	SSD density (kN/m ³)	Oven-dry density (kN/m ³)	Water absorption (%)
Sand	26.87	25.10	24.12	4.20
Gravel (the grains with diameters finer than 2.54 cm sieve)	26.77	24.41	23.04	5.88
Gravel (the grains with diameters coarser than 2.54 cm sieve)	25.69	24.02	22.94	4.65

is surveyed after some F-T cycles. To this end, the scanning electron microscope (SEM) images of the mixtures are prepared and the deterioration of cement paste compounds is investigated.

The MDD and OWC of all mixture designations are determined following the ASTM D558 [35]. According to the standard procedure, the aggregates of native soil are separated into coarse and fine fractions based on passing and retaining on a sieve No. 4. The coarse fraction of the native soil is saturated but the surface of aggregates is dried to achieve the saturated surface dried (SSD) state. The fine fraction of native soil is dried. Then, the predetermined weight of cement is added to the fine fraction of native soil. The dry mixture is carefully blended to make a high degree of uniformity. Next, water is added to the dry admixture, and then the coarse fraction of the native soil in the SSD state is added to the wet admixture to prepare the final state of the mixture. By preparing numerous fresh

mixtures with different water contents, the dry density of the fresh mixture is measured for a range of moisture contents. Then, the OWC and MDD are determined from the dry density-moisture curve.

The test specimens of the UCS test are prepared with the aforementioned procedure, and the fresh mixture with OWC is compacted in a cylindrical mold with a height of 30 cm and a diameter of 15 cm to achieve the maximum density. Then, the samples are cured within the moisture room under a constant room temperature and full humidity condition for two periods of 7 and 28 days. After completing the curing process, the UCS is measured for all mixture designations following the procedure of the ASTM D1633 standard [36]. The loading jack in the UCS test apparatus is controlled by a stress rate of 120 kPa/s which falls within the acceptable range of the ASTM standard.

The hydraulic conductivity of the cemented mixtures is measured in a flexible wall permeameter chamber

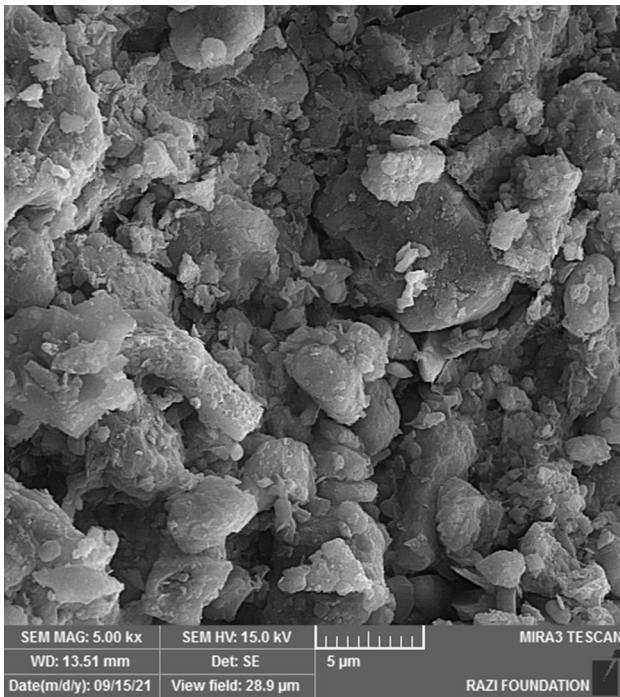


Fig. 4 The scanning electron microscope (SEM) image of soil grains

Table 3 The total chemical compositions (in percent) of cement agent

Si ₂ O	Al ₂ O ₃	Fe ₂ O ₃	CaO	MgO	SO ₃
21.7	4.7	3.6	63.6	3.5	2.9

following the ASTM D5084 standard [37]. The specimen of the hydraulic conductivity test has a cylindrical shape with a diameter of 10 cm and a height of 20 cm and is compacted with maximum density. After curing the samples for two ages of 14 and 27 days by submerging in a water pool, the hydraulic conductivity is measured at these curing ages. During the hydraulic conductivity test, the hardened mixture is covered by a thin latex membrane and installed inside a large-scale cell. Then, the test specimen is saturated by circulating distilled water from the sample bottom to the upper cap. To achieve full saturation in the sample, a back pressure of 200 kPa is kept in the test sample until the test termination. By this method, the target B-value of 95% is adjusted in the sample. In the next step, water under a constant head of 244 mm flows from the sample bottom and the discharge is measured throughout the sample upper cap. Thus, the hydraulic conductivity of the mixture is measured with the constant head method.

The F-T durability of the CSG mixtures is examined following the procedure of ASTM D560 [38]. In this test, two cubic samples with identical conditions are prepared

for each mixture designation and cured inside the moisture room for 7 days. Then, both samples are subjected to 12 cycles of freezing and then thawing. In each cycle, both samples are kept in the freezing box at -23 °C for 24 h. Then, the samples are brought out and kept in the melting condition at 21 °C for 24 h. After each cycle, one sample is brushed with a wire scratch brush, followed by measuring the volume loss of the sample. Besides, the second sample is frequently weighted for measuring weight loss. The weight loss of all mixture designations after each F-T cycle is determined by dividing the difference between the current and the initial weights by the initial weight. To evaluate the effect of the F-T cycles on the mechanical behavior of the CSG mixture, the compressive strength of the mixture with 10% cement content is measured after the 6th, 8th, and 12th cycles and compared with the intact mixture.

3 The key specifications of CSG mixtures

3.1 Compaction test results

The graph of dry density versus moisture content for all CSG mixtures is presented in Fig. 5. Moreover, the graphs of MDD and OWC of mixtures with various cement contents are presented in Fig. 6. The compaction graph of CSG mixtures is separately distinguished in all ranges of water contents, and the mixture with the greater cement content has the higher density at all levels of moisture content. This result implies that the cementing agent facilitates the densification of the fresh mixture in all ranges of water contents. Thus, the MDD and OWC of mixtures are related to the cement content in such a manner that the MDD and OWC increase by increasing the cement content in the mixtures. According to the free-drainage specification of

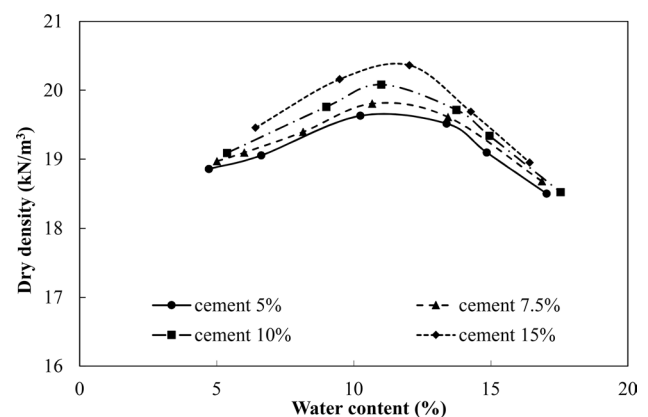


Fig. 5 The dry density–water content graph of CSG mixtures in compaction test

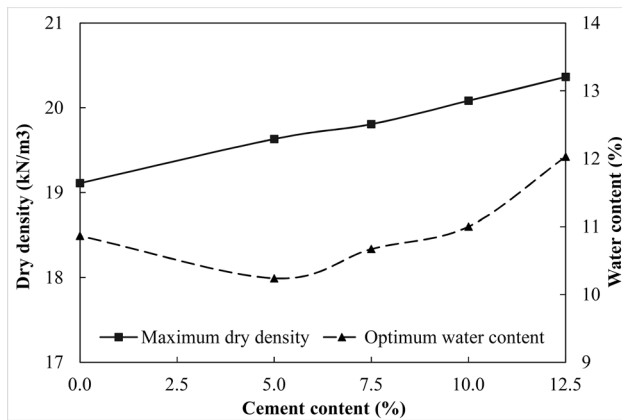


Fig. 6 The graph of MDD and OWC for the CSG mixtures with different cement contents

the native soil (due to less fine-grained content), the maximum compaction state of native soil should be measured with the vibratory method following the standard of ASTM D4253 [39]. However, the compaction test of the native soil is conducted with a similar tamping procedure used for the CSG mixtures to compare the results. The MDD of all CSG mixtures becomes greater than that of the native soil, and the dry density of native soil increases from 19.11 to 20.36 kN/m³ with an increased rate of 6% after blending the native soil with 12.5% cement. In contrast, the OWC of mixtures with low cement becomes lower than that of the native soil. The densification of grains in the mixture is facilitated and the OWC is reduced as the cement paste covers around the native soil grains in the mixture. However, a greater amount of water is required to activate the cement paste after increasing the cement content in the mixtures, and the OWC increases in the mixtures with higher cement content. It should be noted that all CSG mixtures compacted with the OWC withstand in the slump test of concrete (Fig. 7), and thus the fresh mixture is appropriately compacted under a heavy-duty roller in practical conditions.

Based on the compaction test results, the MDD and OWC of the CSG mixtures increase up to 10% by increasing the cement content from 0 to 12.5%, and thus the compaction of the fresh cemented mixture does not considerably depend on the cement content. This consequence was previously observed for the compaction of clay soil treated by cement [40–42].

3.2 Uniaxial compressive strength of mixtures

In contrast to the compaction test, the strength and stiffness of the CSG mixture are directly associated with the cement content. The stress–strain graph of mixtures with different cement contents after a curing age of 28 days is



Fig. 7 The slump test of CSG mixture with 12.5% cement content and in the fresh state

shown in Fig. 8. Besides, the UCS and tangential deformation modulus (measured at a stress level equal to half of UCS) for all samples with different curing ages are presented in Fig. 9. Accordingly, the UCS and deformation modulus gradually increase, and in turn, the ultimate strain decreases by increasing the cement content. The cement content in the mixture influences the general

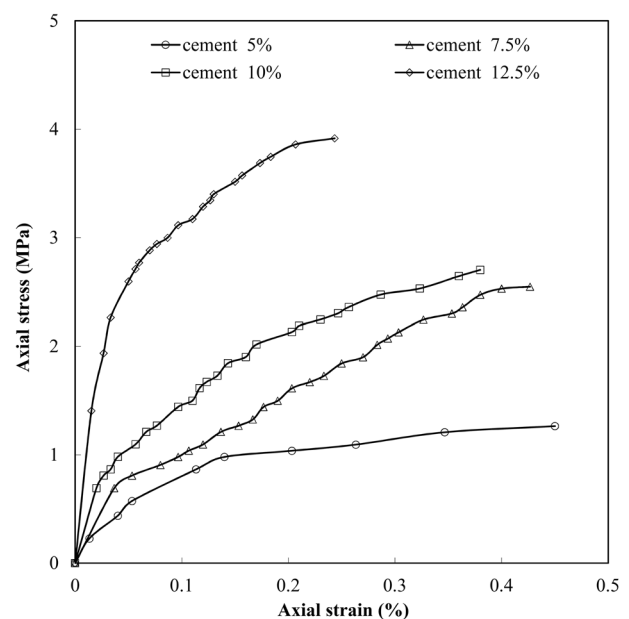


Fig. 8 The axial stress–strain graph for CSG materials with different cement contents after curing age of 28 days

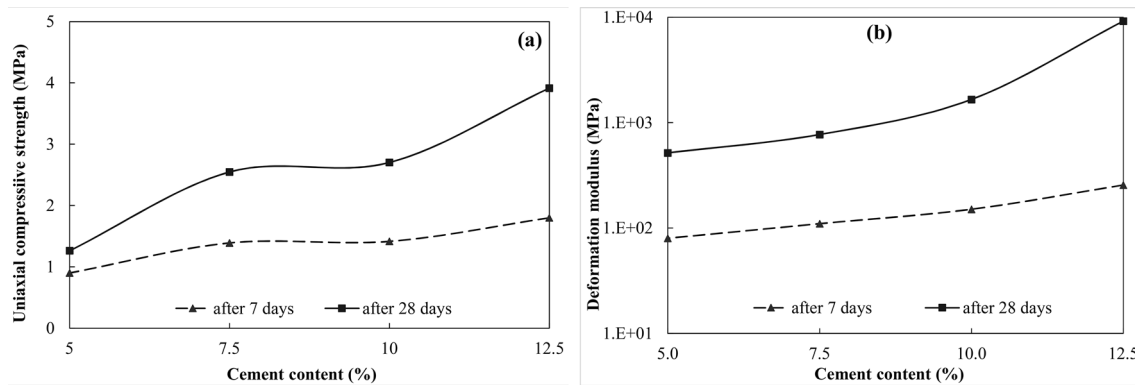


Fig. 9 The graph of uniaxial compressive strength (UCS) (a) and deformation modulus (b) versus cement content for CSG mixtures at two curing ages

shape of the strain–stress graph. When the mixture contains a low cement content of 5%, the test sample shows greater deformation at the early stages of loading. Then, the strain of the sample occurs at a considerable rate at the near-peak stress level. On the other hand, the mixture with the highest cement content of 12.5% exhibits brittle behavior, and limited deformation is observed in the mixture until a stress level equal to half of the peak strength. Then, the deformation of the mixture considerably increases and greater strain is developed in the test sample. The stress–strain graphs of mixtures with cement contents of 7.5 and 10% are similar, and the deformation of test samples gradually occurs at a near-constant rate.

The evolution of compressive strength with the curing age of the CSG mixture is related to the cement content. The curing process of the mixture with 5% cement has less influence on the evolution of strength, and the long-term strength after a curing age of 28 days is raised about 1.38 times compared to the sample with the curing age of 7 days. However, when the mixture contains 12.5% cement, the compressive strength is more enhanced with the curing period, and the strength of the sample with a 28-day curing age is raised about 2.14 times than the sample with 7-day curing age. The effect of curing age is more distinctive in the deformation modulus of mixtures. The rate of increase in the deformation modulus with curing age is directly related to the cement content. The difference of the deformation modulus of the mixture with 5% cement between two curing ages of 28 and 7 days is only 646%. However, the deformation modulus of the sample with 12.5% cement and a 28-day curing age is raised about 37.49 times greater than the sample with a curing age of 7 days. By comparing the deformation modulus and compressive strength of the mixtures with different cement contents between two curing ages, it can be summarized that the resistance and stiffness of mixtures are slowly improved by increasing the cement content in the mixture at the

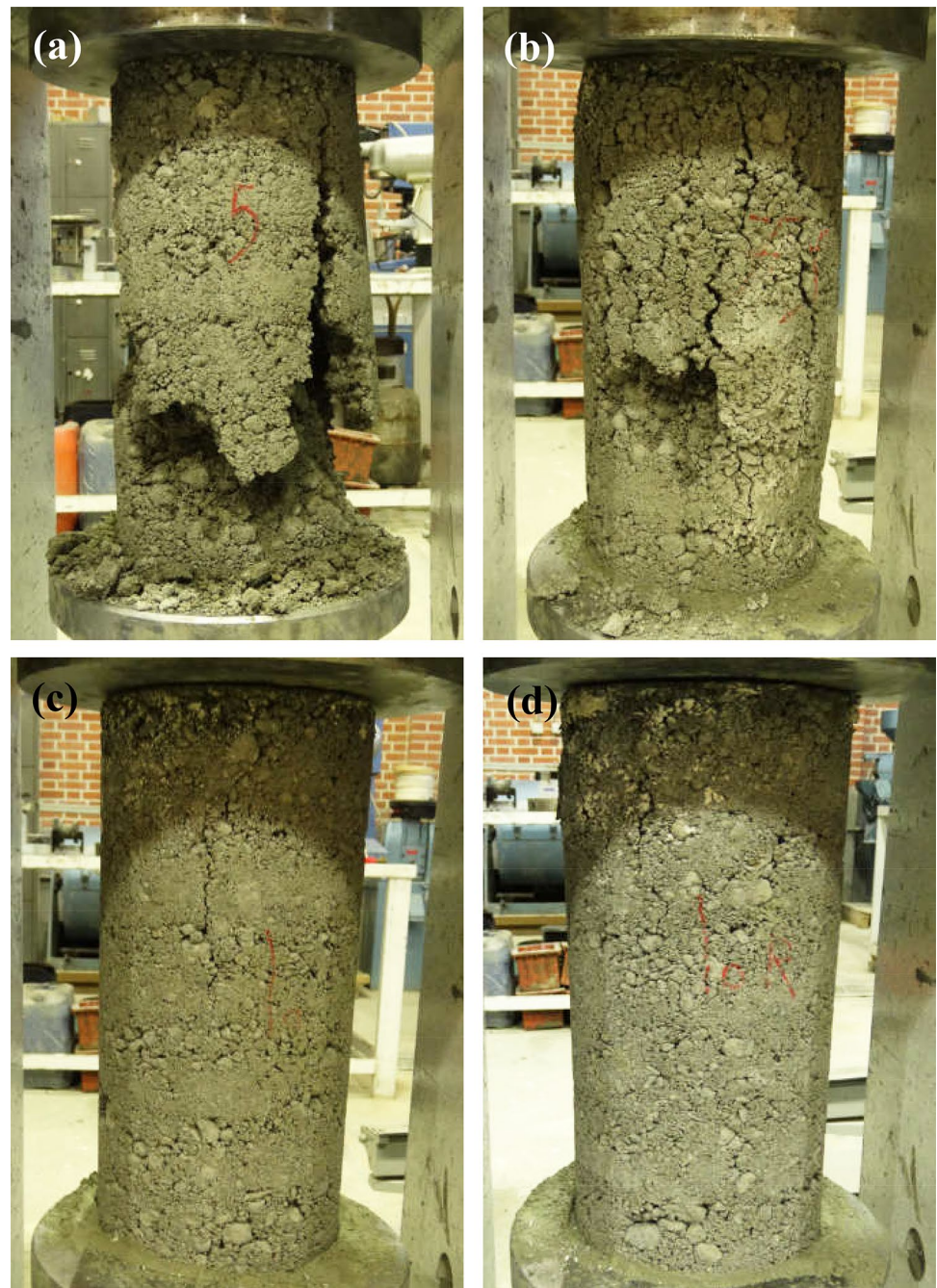
early curing age. However, when the hydration process is completed after 28 days, the resistance and stiffness of the mixture significantly increase with increasing the cement content.

The cement content not only influences the values of strength and stiffness of the CSG mixtures but also governs the failure type of the sample. The failure mode of the mixtures with the cement contents of 5, 7.5, and 12.5% at a curing age of 28 days is shown in Fig. 10. When the mixture has the lowest cement content, the sample bursts under the peak compressive stress, and most of the bonds between the grains that are imposed by the cementation process are broken. Thus, the mixture loses most of the artificial cohesion and tends to show continuous large deformation until reaching the ultimate state. The gradual break of bonding between grains causes a regular increase in sample strains from the early stage of loading, which imposes a ductile behavior in the sample. However, the failure mode of the mixture with 12.5% cement is different from that with low cement. In other words, while the bonding between most of the grains in the mixture with a high cement content is kept in an unbroken condition, a major vertical slip surface is established in the sample under axial loading and causes the sample to fail. Before emerging the slip surface in the sample, the test specimen shows low strains under loading. However, large strains are gradually developed in the sample at the same time with emerging the major slip surface in the sample.

3.3 The hydraulic conductivity of CSG mixtures

The graph of the hydraulic conductivity of the CSG mixture with different cement contents cured at two ages of 14 and 28 days is shown in Fig. 11. Furthermore, the permeability of pure sand with no cementing agent is shown in this figure which is measured via a rigid wall chamber of permeameter following the standard of ASTM D5856

Fig. 10 The failure mode of CSG material in uniaxial compression test at the age of 28 days; **a** 5% cement, **b** 7.5% cement, **c** 10% cement, **d** 12.5% cement



[43]. The cementing agent not only imposes a cohesion between grains and improves the strength of the mixture but also fills the void volume within the mixture, and reduces the permeability of the CSG mixture. The descending trend of the mixture permeability with the cement content exists in both curing ages. However, the intensity of the cementing agent's impact on the permeability reduction is more characteristic in the mixture with an age of 28 days than the curing age of 14 days. For instance, the permeability declines from 9.48×10^{-4} cm/s

to 9.64×10^{-5} cm/s by increasing the cement content from 0 to 12.5% at the curing age of 14 days. To compare the effect of the cement content on the permeability of the CSG mixtures, the permeability of the CSG mixture with a specific cement content is divided by that of the pure native soil that is not blended with cement, which is called the ratio of permeability. The ratio of permeability parameter is used to compare the efficiency of cement for reducing the permeability of the CSG mixture. The ratio of permeability of the CSG mixture with 12.5% cement to the

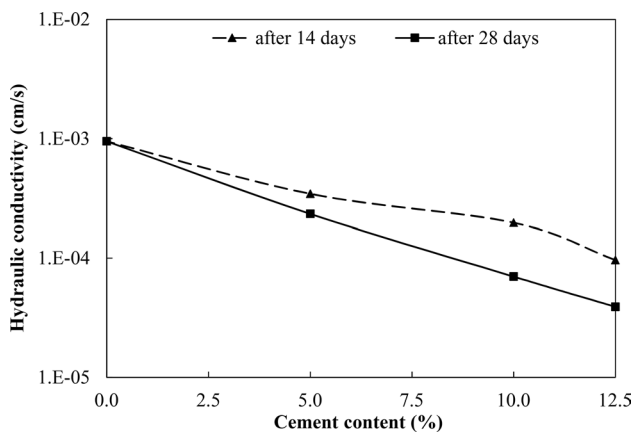


Fig. 11 The permeability graph of CSG material with different cement content after ages of 14 and 28 days

permeability of the untreated native soil becomes about 0.102. Besides, the ratios of permeability of the mixtures with the cement contents of 5% and 10% at a curing age of 14 days to the permeability of untreated native soil are 0.363 and 0.208, respectively. In contrast, the ratios of permeability of CSG mixtures with cement contents of 5%, 10%, and 12.5% after a curing age of 28 days to the permeability of the untreated native soil reduce to 0.247, 0.074, and 0.041, respectively. This fact implies that the efficiency of the cementing agent in the reduction of mixture permeability is improved after hardening the cemented mixture, and more pore spaces in the mixture are blocked by the cement gel after completing the hydration process.

4 Durability of the CSG mixtures

4.1 Freeze–thaw durability of native soil grains

For examining the durability of CSG mixtures, the durability of individual aggregates of the native soil against the F-T cycles is examined with method A introduced in the AASHTTO T-103 procedure [44]. In this test, the dried aggregates are separated on the specified sieves, and the initial weight of retaining on the *i*th sieve is measured and denoted by B_i . After immersing the grains inside the water, the fully submerged aggregates are subjected to 50 cycles of F-T. After completing all F-T cycles, the soil aggregates were dried and passed through the identical sieves again, followed by weighting the retaining on *i*th sieve (denoted by C_i for each sieve). The weight loss percentage of separate aggregates on each sieve is calculated by subtracting the final and initial weight of retaining on the *i*th sieve and dividing by the initial retaining weight (i.e. $D_i = \frac{B_i - C_i}{B_i} \times 100$). The total weight loss of both gravel and sand fractions of native soil are separately calculated by the following equation.

$$E = \sum (D_i) * \frac{(A_i - A_{i-1})}{\text{Gravel or sand fraction percentage in initial native soil}} \tag{1}$$

where the $(A_i - A_{i-1})$ is the difference of the retaining percentage of initial soil between two sequent sieves. The sand and gravel fractions are referred to as the passed and retained on a No. 4 sieve, respectively.

The weights of the aggregates retaining on the various sieves before and after the latest cycle of F-T are presented in Table 4. Moreover, the calculated weight loss for both gravel and sand fractions is presented in this table. As seen, the aggregates exhibit considerable weight loss after

Table 4 The result of freeze–thaw test for the native soil aggregates

	Sieve size (mm)	Initial passing percent (%) (A)	Weight of soil grains retaining on each sieve			Calculated total weight loss percentage of each fraction (%) (E)
			Before test (B) (gr)	After test (C) (gr)	Weight loss for retaining on each sieve (D=(C-B)/B × 100) (%)	
Coarse fraction (gravel)	19	100.0	0	0	0.0	14.34
	12.5	62.2	674	674	0.0	
	9.5	43.7	330	330	0.0	
	4.75	26.9	300	113	62.3	
Fine fraction (sand)	2.36	20.2	120	55	54.2	69.17
	1.18	13.5	120	19	84.2	
	0.6	6.7	120	27	77.5	
	0.3	0.0	120	47	60.8	
Passing through No. 60 sieve (0.3 mm)		0	0	519		

50 cycles of F-T. Even though the maximum acceptable limit for F-T loss of aggregates for use in the road embankment is restricted to 10%, the gravel and sand aggregates lost about 14% and 69% of their original weights due to fragmentation and splitting, and the majority of soil grains are transformed to small-size grains passed through the No. 60 sieve. Thus, the soil aggregates are severely damaged after frequent F-T cycles. This fact implies the weak nature and low resistance of the original coarse-grained sand soil under the environmental effect, especially the frost-thaw event. To utilize this soil in the embankment, therefore, the durability of native soil under the F-T effect is improved by blending with cement additive.

4.2 Freeze–thaw durability of the CSG mixtures

The weight loss graph of the CSG mixtures under the F-T cycles is plotted in Fig. 12a. The weight of all mixtures decreases as they undergo the F-T cycles. However, the rate of weight loss with proceeding with the F-T cycles completely depends on the cement content of mixtures. The weight-loss trend of the mixtures with 5 and 7.5% cement is similar, and the deterioration of mixtures occurs at a similar intensity in all F-T cycles. However, when the cement content increases in the mixture, the form of the weight loss graph fairly differs. The weight loss graph for the mixtures with a cement content greater than 10% has a bilinear form, and the rate of the weight loss varies after the 4th cycle. In earlier F-T cycles, samples deteriorate at a comparatively fast rate and the weight loss graph has a greater slope. However, the rate of weight loss decreases after the 4th cycle, and the graph tends to the near horizontal slope. The reason for the change in the weight loss rate may be the completion of the hydration process in the mixtures with greater cement content. As thought in the interpretation of the results of the uniaxial compression test, the strength of the mixture with a high cement content significantly increases with the curing time as

the hydration process, and the cementation bonding between grains is mostly completed. This phenomenon is responsible for reducing weight loss after advancing a specific cycle of F-T. A similar consequence was observed in the F-T durability test of the clay soil stabilized with the cement, where the degradation rate of the cemented clay soil decreased after the 5th cycle of F-T [8]. Moreover, de Jesús Arrieta Baldovino et al. [45] reported that characteristic loss of mass of cemented silty sand in F-T test considerably decreased after 5th cycle of F-T. This trend was observed in mixtures with different cement contents and compaction degree. However, the reduction rate of mass loss after 5th cycle of F-T is more distinctive in mixture with low cement content.

The volume change of samples after each cycle of F-T is shown in Fig. 12b. The irregular shape of the volume change graph in all mixtures may be referred to as the irregular shape of mixtures after each step of brushing which imposes a discrepancy in the volume measurement of samples. The cement content in the mixture has a significant influence on the volume change graph. All samples exhibit expansion at earlier stages of F-T. Then, the volume of samples declines the degradation of the samples after the last cycles, and the dimensions of samples decrease under the brushing action. The main cause of the initial expansion of the CSG mixture at early cycles of F-T may be referred to as the absorption and movement of moisture within the cemented mixture at the thawing part of the cycle. The investigations of Ishikawa et al. [46] indicated the movement of moisture from the grain inside to the grain surface of cemented sands during the thawing phase in early F-T cycles. The moisture migration in soil grains in the thawing phase increases the free water content on the particle surface caused by freeze–thaw. In the next F-T cycles, the soil structure is deteriorated by the frost expansion of pore water in the surface leading to a decrease in the sample volume due to the separation of the grains from the cemented mixture surface. The initial

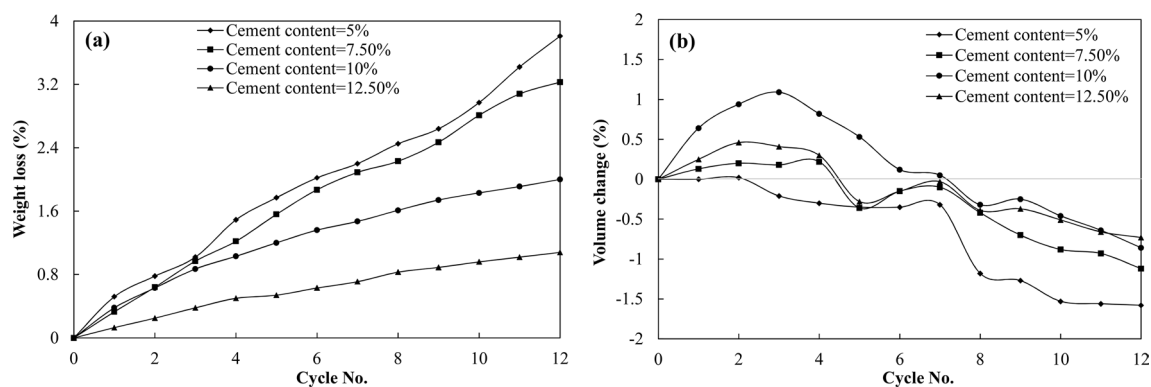


Fig. 12 The weight loss **(a)** and volume loss **(b)** of CSG mixtures after freezing–thawing cycles

expansion behavior is more considerable in the mixtures with a high cement content and, in turn, the volume reduction during the latest cycles is found with greater intensity in the mixtures with less cement content. The mixture with a cement content of 5% showed very slight expansion in earlier F-T cycles, and in turn, the greatest volume reduction occurred in this mixture due to the deterioration in the last F-T.

The final results of the F-T test for all mixtures which is thought as the weight loss percentage after the 12th cycle are presented in Table 5. As with the uniaxial compression test result, the F-T resistance of mixtures with cement contents of 5 and 7.5% becomes close and similar. However, the mixture with 12.5% cement has the greatest resistance against the F-T effect.

5 Some considerations on the durability of the CSG mixtures

The F-T test result of native soil indicates that the individual aggregate grains are effortlessly broken under F-T cycles. However, the durability of stabilized coarse-grained soil under the frost-thaw effect is improved after blending with the cementing agent. According to the total weight loss of CSG mixtures after 12 cycles of F-T (Table 5), the weight loss due to F-T becomes below 5% for all mixtures. This value is the threshold limit for the soil–cement mixture to be used as an upstream protection layer in the embankment [47]. The upstream protection layer is employed to withstand the high waves of the dam reservoir and should be robust against the severe environmental effect. When the CSG material satisfies the requirements for the protection layer of earthfill dams, this type of stabilized soil can be employed as the filling material of hardfill embankments. However, the sequence cycles of F-T can impose a noticeable weakness in the mechanical performance and microstructure of the cemented material inside the dam body. To this end, the uniaxial compressive test is conducted on three samples of the CSG mixture with 10% cement that undergoes the 6th, 8th, and 12th cycles of F-T. The UCS values of these samples under 6, 8, and 12 cycles of F-T are measured as 2.32, 2.12, and 1.73 MPa, respectively. The intact mixture, which does not experience any F-T cycle, has a UCS of 2.702 MPa. Comparing the result indicates that the sequence cycles of the F-T

event reduce the strength of the CSG mixture in order of 14%, 21.5%, and 36% after the 6th, 8th, and 12th cycles of F-T, respectively. A descending trend is observed for the deformation modulus, and after the same number of F-T cycles, the deformation modulus decreases about 24, 30, and 41%, respectively. A similar decreasing trend was reported for the strength of other cemented soils after F-T cycles.

To investigate the effect of the F-T cycles on the performance of the CSG mixtures, the microstructure of the CSG mixture with 10% cement is analyzed after encountering 6, 8, and 12 cycles of F-T, and the scanning electron microscope (SEM) images of the mixtures are shown in Figs. 14, 15 and 16, respectively. Besides, the microstructure of the intact CSG mixture (with no F-T cycle) is shown in Fig. 13. By completing the hydration process in the CSG mixtures at an earlier time, some new products such as Portlandite (calcium hydroxide (CH) with a chemical formula of Ca(OH)_2), initial ettringite, CSH (calcium-silicate-hydration), and other complexes are emerged within the hardened Portland cement pastes [48]. The initial ettringite emerges in the intact mixture after the initial hydration phase in the mixture and appears as a form of the long and narrow needle shape (Fig. 13b) [49]. Portlandite is another hydration product that is exhibited as a hexagonal thin sheet in the SEM images of the CSG mixture (Fig. 13b) [49]. CSH is one of the key products of the cement hydration process that is responsible for bonding and strength evolution in concrete or soil stabilized by cement [50]. The CSH is exhibited in the form of sheet and honeycomb, which are detected with high brightness in the SEM image (Fig. 13a). As the CSH compound fills the internal voids of hydrated cement paste, the brightness of the CSH compounds in the SEM image increases [48]. Any change in these formations of the cement hydration product may lead to changes in the strength and structure of the CSG mixture.

It was concluded from previous research [21, 25] that the main reason for damage in the cemented soils and concrete during the F-T cycles is referred to as a physical action of icing expansion within air voids. However, the current investigation demonstrates the severe damage in the hydrated cement paste after the F-T cycle. When the CSG mixture undergoes the F-T cycles, the formation and intensity of hydration products vary, and these formations are decomposed into other elements. After the CSG mixture experiences six cycles of F-T, the initial ettringites

Table 5 The freeze–thaw test result for CSG mixtures

Mixture designation	Mixture #1	Mixture #2	Mixture #3	Mixture #4
Cement content	5%	7.50%	10%	12.50%
Weight loss percent after 12 freeze–thaw cycles	3.89	3.31	1.86	0.95

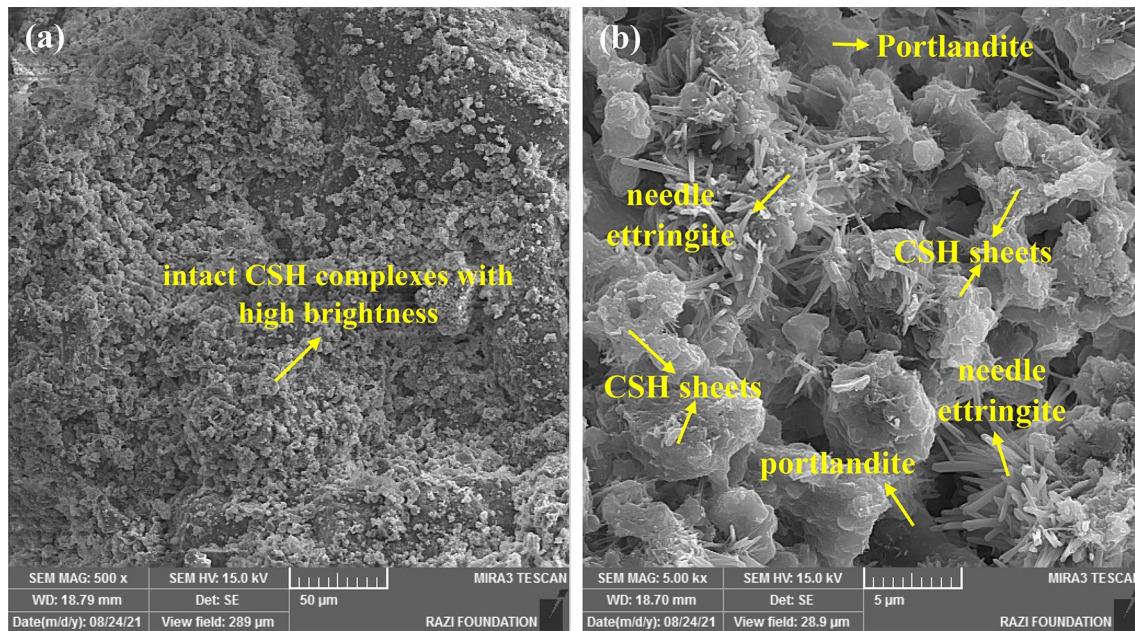


Fig. 13 The scanning electron microscope (SEM) images of intact mixture with 10% cement and no F-T cycle: **a** 500× magnification, **b** 5000× magnification

are disintegrated and their size and intensity are reduced (Fig. 14b and c). The stability of initial ettringites and monosulfate in the cemented soils and concrete depends on the internal temperature and pH of the mixture [51]. When the cemented soil is subjected to a very low temperature during the freezing phase, the initial ettringites and monosulfate phases are decomposed in the CSG mixture (Fig. 14b, c), and the SO_4^{2-} ion is released from the ettringites. This issue was firstly observed in concrete by Stark et al. [52] and Stark [53]. The breakdown of initial ettringite is observed in the mixtures subjected to the 8th and 12th cycles (Figs. 15b, 16b).

After decomposition of the initial ettringites and monosulfate in the mixture, the F-T cycles primarily influence the CSH compound and most CSH compounds are disintegrated. As seen in the SEM image of the mixture under the 6th cycle (Fig. 14a), the intensity and the extension of bright honeycomb sheets of CSH decreased. The degradation of the CSH compound is progressively intensified in the next cycles of F-T, and a low quantity of the CSH compounds with high brightness is detected in the mixture under the 8th F-T cycle (Fig. 15a) and the 12th F-T cycle (Fig. 16a). When the sulfate ion is released after decomposing the initial ettringites within the mixture due to the F-T cycle, this free sulfate ion attacks on the CSH compounds and the Ca^{2+} ions of the CSH compound are released. Collepari [54] showed a similar sulfate attack on the CH and CSH compounds in the conventional concrete, which leads to producing gypsum and delayed ettringite.

Thus, the CSH complex is weakened in the mixture after F-T cycles. This issue can be found in the EDX analysis of SEM images (Table 6). After degradation of CSH, the amount of Ca^{2+} ion gradually increases in the next F-T cycles, and all mixtures subjected to F-T cycles have higher Ca^{2+} ions than the intact mixture. The free sulfate ion combined with the accessible moisture and some amount of Ca^{2+} ions in the mixture produced the gypsum and delayed ettringites. The delayed ettringite plays a destructive role in the cemented mixture and can accelerate the sulfate attack in the cemented soil and concrete [54, 55]. The gypsum is mainly observed in the form of a dark sheet [56] around the initial ettringites. This phenomenon is shown in Figs. 14c, 15c, and 16c for the mixtures under the 6th, 8th, and 12th cycles of the F-T, respectively. A similar emergence of delayed ettringite was previously observed in the other cemented soil subjected to the F-T cycles [25].

At the same time with diminishing the CSH and initial ettringite in the mixture subjected to F-T cycles, some new micro-cracks have emerged within the C_3A compound of the hydrated paste. Besides, considerable new pore spaces are developed within the cement paste. The C_3A compound is another product of decomposition of initial ettringite that is detected in the form of a dark cube that mainly occupies the cemented paste [54, 56]. Furthermore, the disintegration of initial ettringite and monosulfate compounds leads to the release of the interlayered water retained inside the hydration paste [52–54]. This moisture is kindly transformed into

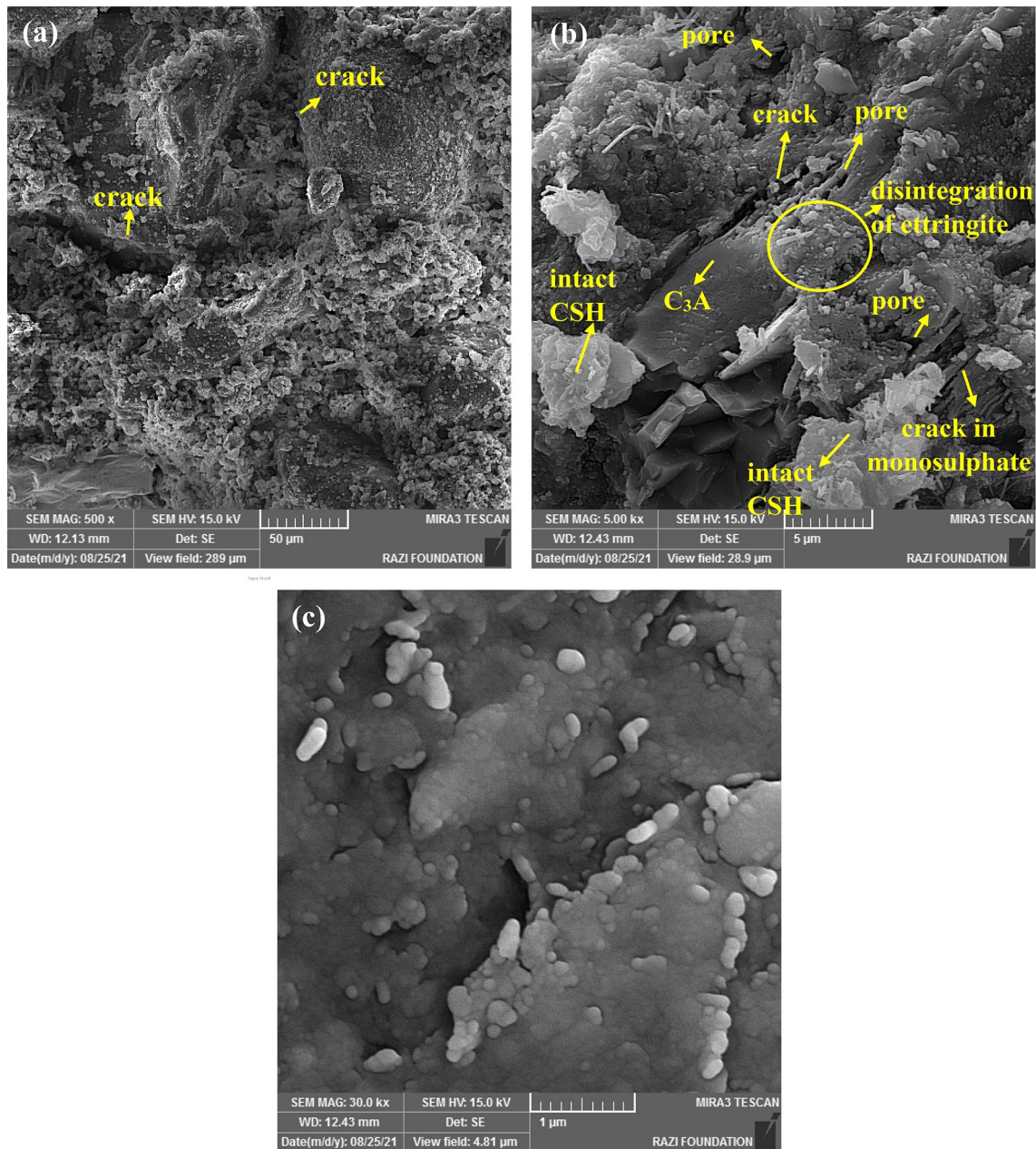


Fig. 14 The scanning electron microscope (SEM) images of mixture with 10% cement subjected to the 6th F-T cycle: **a** 500× magnification, **b** 5000× magnification, **c** 30,000× magnification

free water and migrates from the hydrated paste to the void space of the mixture. When the free water and other prevailing moistures (which are mainly migrated from the soil grains at thaw phase [46]) are frozen during the freezing stage of the F-T cycle, the extra volume of ices inside the pore space imposes new micro-cracks inside the C_3A compound of cement paste. The size of these new void spaces is very limited in the earlier 6th cycle of F-T (Fig. 14b). As the mixture suffers further cycles of F-T, the extension and number of micro-cracks increase

(Fig. 15b). At the 12th F-T cycle, a long crack with considerable width is observed (Fig. 16b). These cracks introduce a weakness in the structure of cemented mixture and reduce the strength of the mixture. Developing micro-cracks were observed in other cemented soils encountering F-T cycles [22]. Besides, de Jesús Arrieta Baldovino et al. [45] postulated that F-T cycles weakened the cement hydrated paste in the cemented soil which have a negative impact on the filling in soil pores and bonding between grains.

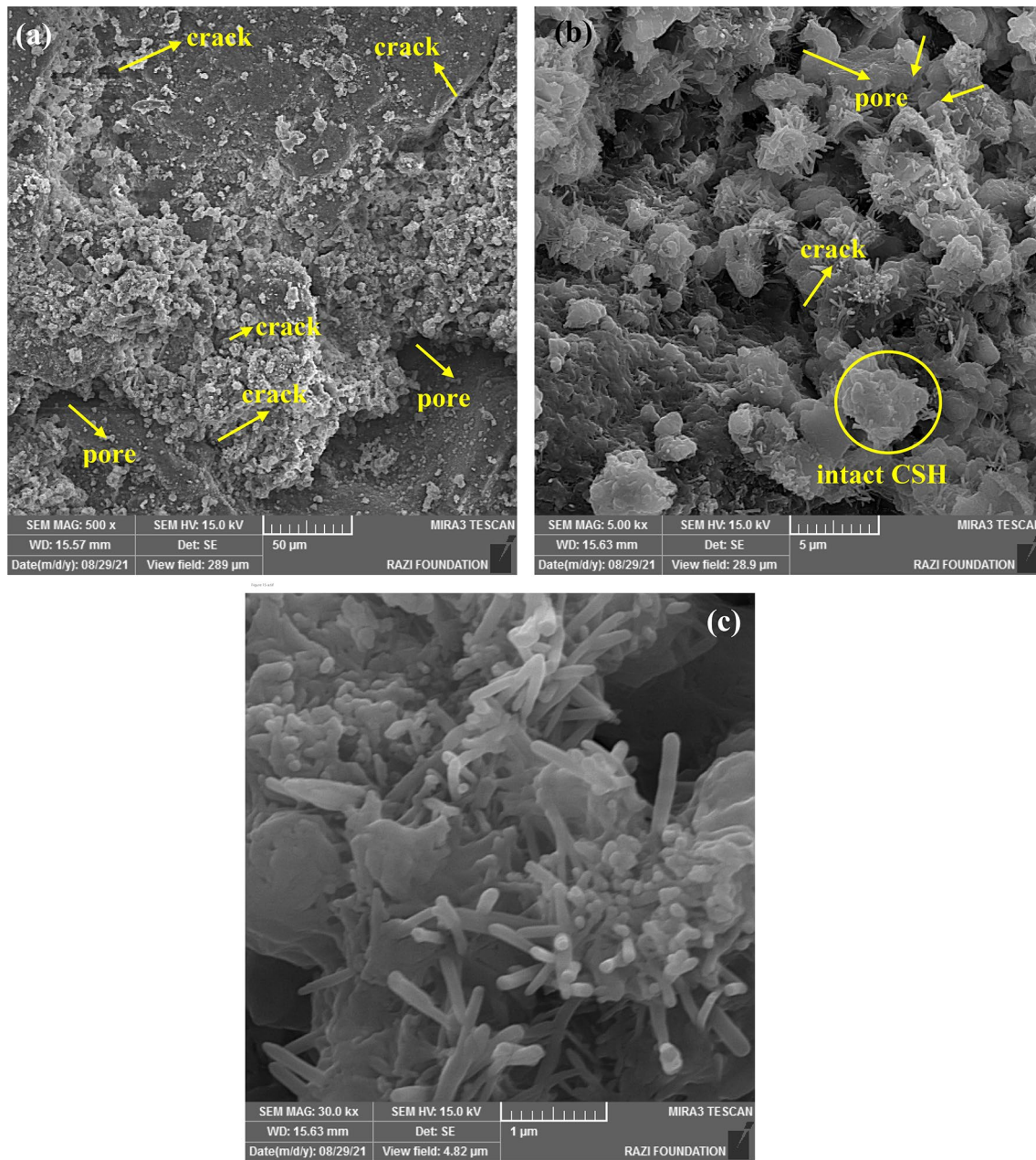


Fig. 15 The scanning electron microscope (SEM) images of mixture with 10% cement subjected to the 8th F-T cycle: **a** 500× magnification, **b** 5000× magnification, **c** 30,000× magnification

The analyses of SEM images of the CSG mixture subjected to various F-T cycles imply that four factors including disintegration of the CSH complex, imposing new pore space and micro-cracks, releasing free water, and establishing the secondary ettringite and gypsum

are the main reasons that reduce the strength and stiffness of the CSG mixtures after encountering to the F-T cycles.

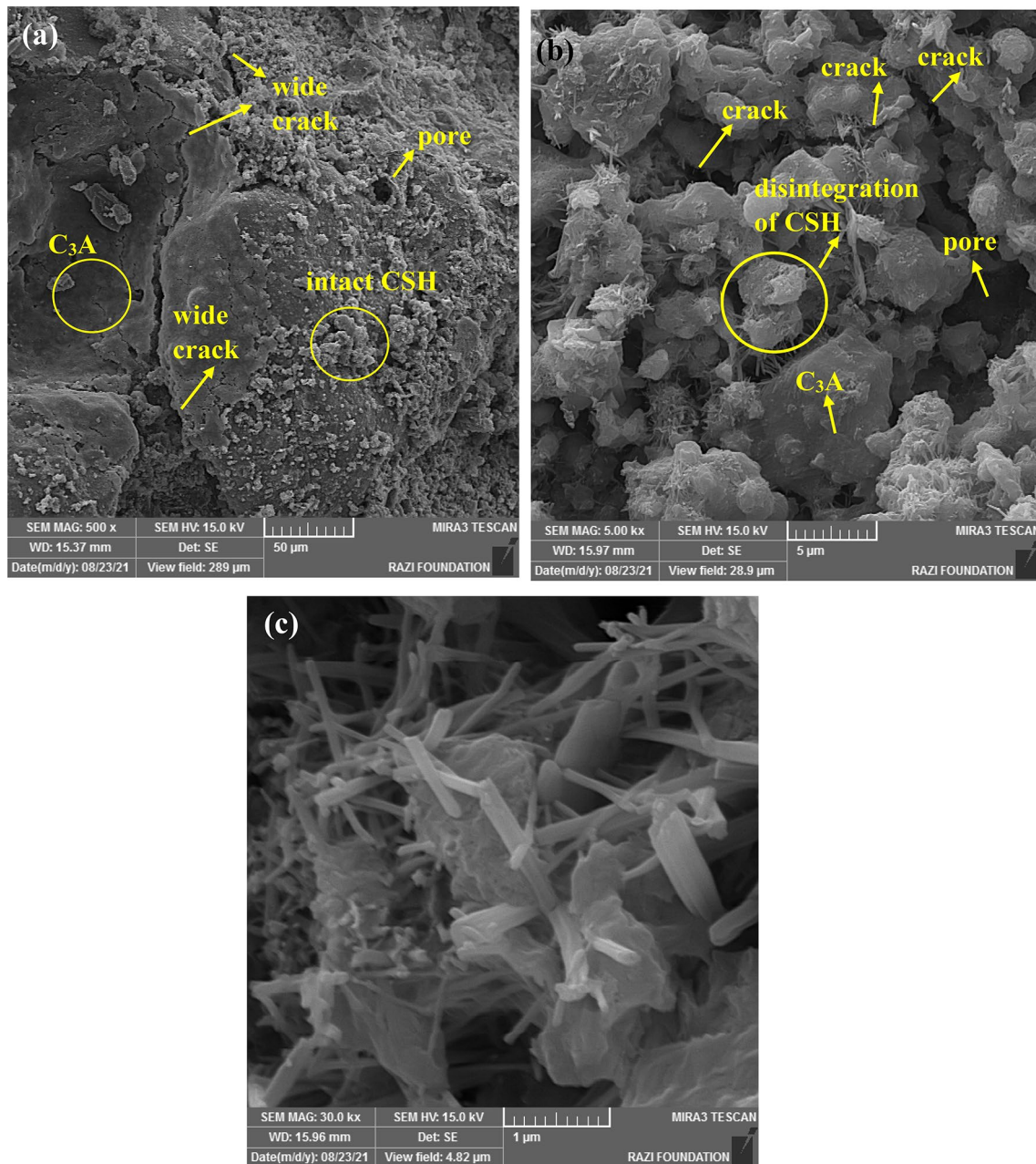


Fig. 16 The scanning electron microscope (SEM) images of mixture with 10% cement subjected to the 12th F-T cycle: **a** 500× magnification, **b** 5000× magnification, **c** 30,000× magnification

6 Conclusion

The freeze–thaw durability, permeability, and compressive strength of cemented sand-gravel mixtures were investigated in this paper. The test results can be summarized as follows:

- The compaction test results are not significantly influenced by the cement content of mixtures. However,

the MDD and OWC slightly increase by increasing the cement content. These results can be expected in many cemented soils.

- The result of the UCS test is completely related to the cement content that is confirmed by previous studies. The mixture with a greater cement content shows higher strength and greater deformation modulus and exhibits brittle behavior with small ultimate

Table 6 The quantitative results of EDX-SEM analysis including the weight percentage of basic elements in the bulk of the CSG mixture with 10% cement encountering various F-T cycles

Element	Intact mixture	6th cycle of F-T	8th cycle of F-T	12th cycle of F-T
C	16.09	23.33	19.28	11.95
O	50.24	43.78	46.86	49.64
Na	0.92	0.3	0.52	0.52
Mg	1.11	0.68	0.77	0.73
Al	3.1	2.49	2.99	3.19
Si	9.05	9.06	10.46	11.68
K	0.79	0.42	0.51	0.58
Ca	14.7	18.12	16.85	20.03
Fe	1.09	1.82	1.76	1.68

strain. Comparable compressive strength is found in mixtures with cement contents of 5 and 7.5%.

- The compressive strength and deformation modulus of the mixture with higher cement are considerably raised in the later curing aging. In turn, the strength and stiffness of the mixture with less cement comparatively increase with a lower rate after the 28-day curing age. This issue can be expected for more general cases of CSG mixtures.
- The aggregates of the native soil in mixtures have high intra-void space. This causes the grains to own a high degree of water absorption and, thus, have a considerable weight loss after being subjected to 50 cycles of the freeze–thaw.
- According to the results of the freeze–thaw test conducted for the specific case of the current research, the weight loss of all mixtures with different cement contents is less than 5%, which is the threshold limit for the soil–cement embankment.
- The freeze–thaw durability of mixtures considered for the case study of the current research directly increases with the cement content. Moreover, in a mixture with higher cement content, the rate of degradation in the freeze–thaw test decreases after the 4th cycle. However, the degradation of the mixture with less cement occurs at a similar rate in all cycles.
- Even though the low resistance of native soil grains during the freeze–thaw test, the resistance, and durability of the soil are improved after stabilization with cement. The compressive strength and durability are similar to mixtures containing cement contents of 5 and 7.5%. However, in the mixtures with cement contents greater than 10% in the current research, the strength and durability increase with increasing cement content.
- According to the microstructure analysis of the mixture, the F-T cycles influence the hydrated cement paste, and the key products of the hydrated cement are decomposed and disintegrated. This issue is a universal con-

clusion that can be generalized for the cemented soils subjected to the F-T cycles.

- In general state, it is recommended that the dam designers should concern about the reduction effect of the frost–thaw event on the mechanical response of hardfill dams. In the current research, the reduction factor of up to 40% is obtained for applying the measured strength of the CSG mixture in normal laboratory conditions to account for the effect of the freeze–thaw event in practical conditions.
- It is strongly suggested to study the F-T durability of the CSG mixtures prepared with different initial conditions in the future. For instance, the curing temperature and aging may affect the durability of the CSG mixtures and should be investigated.

Acknowledgements The current research is conducted under the financial support of East Azarbaijan Organization of Forests, Range and Watershed Management-Iranian ministry of Agriculture-Jahad (Agreement No. 24182-1396/12/20).

Author contributions The authors confirm contribution to the paper as follows: Conceptualization [Hamed Farshbaf Aghajani]; Data curation [Mohammad Salimi, Sina Karimi, Vahid Estekanchi]; Formal analysis, [Mohammad Salimi, Sina Karimi, Vahid Estekanchi, Reza Akbarzadeh Ahari]; Funding acquisition [Reza Akbarzadeh Ahari]; Investigation [Hamed Farshbaf Aghajani, Hossein Soltani-Jigheh]; Methodology [Hamed Farshbaf Aghajani]; Resources [Mohammad Salimi, Sina Karimi, Vahid Estekanchi, Reza Akbarzadeh Ahari]; Supervision [Hamed Farshbaf Aghajani]; Validation [Hossein Soltani-Jigheh]; Visualization [Hossein Soltani-Jigheh, Mohammad Salimi, Sina Karimi]; Writing—original draft [Hossein Soltani-Jigheh, Vahid Estekanchi]; Writing—review & editing [Hamed Farshbaf Aghajani].

Data availability The data that support the findings of this study are available from East Azarbaijan Organization of Forests, Range, and Watershed Management but restrictions apply to the availability of these data, which were used under licence for the current study, and so are not publicly available. Data are however available from the corresponding author upon reasonable request and with permission of East Azarbaijan Organization of Forests, Range, and Watershed Management.

Declaration

Conflict of interest The authors declare no conflict of interest.

Open Access This article is licensed under a Creative Commons Attribution 4.0 International License, which permits use, sharing, adaptation, distribution and reproduction in any medium or format, as long as you give appropriate credit to the original author(s) and the source, provide a link to the Creative Commons licence, and indicate if changes were made. The images or other third party material in this article are included in the article's Creative Commons licence, unless indicated otherwise in a credit line to the material. If material is not included in the article's Creative Commons licence and your intended use is not permitted by statutory regulation or exceeds the permitted use, you will need to obtain permission directly from the copyright holder. To view a copy of this licence, visit <http://creativecommons.org/licenses/by/4.0/>.

References

1. Yokotsuka T (2000) Application of CSG method to construction of gravity dam. *ICOLD 2000 at Beijing* 4(14)
2. Jia J, Lino M, Jin F, Zheng C (2016) The cemented material dam: a new, environmentally friendly type of dam. *Engineering* 2(4):490–497. <https://doi.org/10.1016/J.ENG.2016.04.003>
3. Londe P, Lino M (1992) The faced symmetrical hardfill dam: a new concept for RCC. *Int Water Power Dam Constr* 44(2):19–24
4. Cai X, Wu Y, Guo X, Ming Y (2012) Research review of the cement sand and gravel (CSG) dam. *Front Struct Civ Eng* 6(1):19–24. <https://doi.org/10.1007/s11709-012-0145-y>
5. Batmaz S (2003) Cindere dam-107 m high roller compacted hardfill dam (RCHD) in Turkey. *Roller Compacted concrete Dams*, pp 121–126
6. Guillemot T, Lino M (2012) Design and construction advantages of hardfill symmetrical dams-case study: SafSaf Dam In Eastern Algeria. *Zaragoza* 23:25
7. Jia J, Ding L, Wu Y, Li A, Li S (2020) Building cemented material dam with soft rock material. In: *The international conference on Embankment dams*. Springer, pp 27–35. doi:https://doi.org/10.1007/978-3-030-46351-9_3
8. Ding M, Zhang F, Ling X, Lin B (2018) Effects of freeze-thaw cycles on mechanical properties of polypropylene Fiber and cement stabilized clay. *Cold Reg Sci Technol* 154:155–165. <https://doi.org/10.1016/j.coldregions.2018.07.004>
9. Justin P, Robert L (2004) Performance of soil stabilization agents. K-TRAN: KU-01–8, Department of Transportation, The University of Kansas
10. Olgun M (2013) The effects and optimization of additives for expansive clays under freeze–thaw conditions. *Cold Reg Sci Technol* 93:36–46. <https://doi.org/10.1016/j.coldregions.2013.06.001>
11. Pardini G, Guidi GV, Pini R, Regüés D, Gallart F (1996) Structure and porosity of smectitic mudrocks as affected by experimental wetting—drying cycles and freezing—thawing cycles. *CATENA* 27(3–4):149–165. [https://doi.org/10.1016/0341-8162\(96\)00024-0](https://doi.org/10.1016/0341-8162(96)00024-0)
12. Shihata S, Baghdadi Z (2001) Simplified method to assess freeze-thaw durability of soil cement. *J Mater Civ Eng* 13(4):243–247. [https://doi.org/10.1061/\(ASCE\)0899-1561\(2001\)13:4\(243\)](https://doi.org/10.1061/(ASCE)0899-1561(2001)13:4(243))
13. Thompson MR, Dempsey BJ (1970) Quantitative characterization of cyclic freezing and thawing in stabilized pavement materials. *Highway Research Record* (304)
14. Chai M, Zhang H, Zhang J, Zhang Z (2017) Effect of cement additives on unconfined compressive strength of warm and ice-rich frozen soil. *Constr Build Mater* 149:861–868. <https://doi.org/10.1016/j.conbuildmat.2017.05.202>
15. Li L, Shao W, Li Y, Cetin B (2015) Effects of climatic factors on mechanical properties of cement and fiber reinforced clays. *Geotech Geol Eng* 33(3):537–548. <https://doi.org/10.1007/s12076-014-9838-4>
16. Solanki P, Zaman M, Khalife R (2013) Effect of freeze-thaw cycles on performance of stabilized subgrade. In: *Sound Geotechnical Research to Practice: Honoring Robert D. Holtz II*. pp 566–580
17. Gao C, Du G, Guo Q, Zhuang Z (2020) Static and dynamic behaviors of basalt fiber reinforced cement-soil after freeze-thaw cycle. *KSCE J Civ Eng* 24(12):3573–3583. <https://doi.org/10.1007/s12205-020-2266-5>
18. Wu Y, Qiao X, Yu X, Yu J, Deng Y (2021) Study on properties of expansive soil improved by steel slag powder and cement under freeze-thaw cycles. *KSCE J Civ Eng* 25(2):417–428. <https://doi.org/10.1007/s12205-020-0341-6>
19. Lu Y, Liu S, Zhang Y, Li Z, Xu L (2020) Freeze-thaw performance of a cement-treated expansive soil. *Cold Reg Sci Technol* 170:102926. <https://doi.org/10.1016/j.coldregions.2019.102926>
20. Ding L-Q, Vanapalli SK, Zou W-L, Han Z, Wang X-Q (2021) Freeze-thaw and wetting-drying effects on the hydromechanical behavior of a stabilized expansive soil. *Constr Build Mater* 275:122162. <https://doi.org/10.1016/j.conbuildmat.2020.122162>
21. Chen S, Zheng Y (2018) Study on the evolutionary model and structural simulation of the freeze-thaw damage of cemented sand and gravel (CSG). *J Inst Eng* 99(4):699–704. <https://doi.org/10.1007/s40030-018-0319-2>
22. Jamshidi RJ, Lake CB, Barnes CL (2014) Examining freeze/thaw cycling and its impact on the hydraulic performance of cement-treated silty sand. *J Cold Reg Eng* 29(3):04014014. [https://doi.org/10.1061/\(ASCE\)CR.1943-5495.0000081](https://doi.org/10.1061/(ASCE)CR.1943-5495.0000081)
23. Theivakularatnam M, Gnanendran CT (2015) Durability of lightly stabilised granular material subjected to freeze-thaw and wet-dry cycles. *IFCEE* 2015:1410–1419
24. Li J, Wang F, Yi F, Wu F, Liu J, Lin Z (2019) Effect of freeze-thaw cycles on triaxial strength property damage to cement improved aeolian sand (CIAS). *Materials* 12(17):2801. <https://doi.org/10.3390/ma12172801>
25. Jamshidvand S, Ardakani A, Kordnaei A (2021) Effect of cement and zeolite on silty sand samples under freeze–thaw cycles. *Road Mater Pavement Des*. <https://doi.org/10.1080/14680629.2021.1924238>
26. Kou H-I, Liu J-h, Guo W, Hua S-d, Pan Y-t (2021) Effect of freeze–thaw cycles on strength and ductility and microstructure of cement-treated silt with polypropylene fiber. *Acta Geotech* 16(11):3555–3572. <https://doi.org/10.1007/s11440-021-01325-3>
27. Lu L, Ma Q, Hu J, Li Q (2021) Mechanical properties, curing mechanism, and microscopic experimental study of polypropylene fiber coordinated fly ash modified cement-silty soil. *Materials* 14(18):5441. <https://doi.org/10.3390/ma14185441>
28. Tao Z, Zhang Y, Chen X, Gu X (2022) Effects of freeze-thaw cycles on the mechanical properties of cement-fiber composite treated silty clay. *Constr Build Mater* 316:125867. <https://doi.org/10.1016/j.conbuildmat.2021.125867>
29. Liu H, Sun S, Wei H, Li W (2021) Effect of freeze-thaw cycles on static properties of cement stabilised subgrade silty soil. *Int J Pavement Eng*. <https://doi.org/10.1080/10298436.2021.1919306>
30. ShahriarKian M, Kabiri S, Bayat M (2021) Utilization of zeolite to improve the behavior of cement-stabilized soil. *Int J Geosynth Ground Eng* 7(2):35. <https://doi.org/10.1007/s40891-021-00284-9>

31. ASTM D698 (2007) Standard test methods for laboratory compaction characteristics of soil. Annual book of ASTM standards American Society for Testing and Materials, West Conshohocken, PA
32. ASTM C131 (2006) Standard test method for resistance to degradation of small-size coarse aggregate by abrasion and impact in the Los Angeles machine. Annual book of ASTM standards American Society for Testing and Materials, West Conshohocken, PA
33. ASTM C127 (2004) Standard test method for density, relative density (specific gravity), and absorption of coarse aggregate. Annual book of ASTM standards American Society for Testing and Materials, West Conshohocken, PA
34. ASTM C128 (2004) Standard test method for density, relative density (specific gravity), and absorption of fine aggregate. Annual book of ASTM standards American Society for Testing and Materials, West Conshohocken, PA
35. ASTM (1996) ASTM D558, Standard test methods for moisture-density relations of soil-cement mixtures. American Society for Testing and Materials. Annual Handbook, vol 5. West Conshohocken, PA
36. ASTM (2007) ASTM D1633 Standard test methods for compressive strength of molded soil-cement cylinders, ASTM International, West Conshohocken, PA, USA. American Society for Testing and Materials. Annual Handbook. West Conshohocken, PA
37. ASTM (1990) ASTM D5084 Standard test method for measurement of hydraulic conductivity of saturated porous materials using a flexible wall permeameter. American Society for Testing and Materials. Annual Handbook, vol 4. West Conshohocken, PA
38. ASTM D560 (2003) Standard test methods for freezing and thawing compacted soil-cement mixtures. West Conshohocken, PA, United States. Annual book of ASTM standards American Society for Testing and Materials, West Conshohocken, PA
39. ASTM D4253 (2002) Standard test method for maximum index density and unit weight of soils using a vibratory table". Annual Book of ASTM Standards. Annual book of ASTM standards American Society for Testing and Materials, West Conshohocken, PA, pp 1–14
40. Mohamedzein YE-A, Al-Rawas AA (2011) Cement-stabilization of sabkha soils from Al-Auzayba, Sultanate of Oman. *Geotech Geol Eng* 29(6):999. <https://doi.org/10.1007/s10706-011-9432-y>
41. Reddy BV, Kumar PP (2011) Cement stabilised rammed earth. Part A: compaction characteristics and physical properties of compacted cement stabilised soils. *Mater Struct* 44(3):681–693. <https://doi.org/10.1617/s11527-010-9658-9>
42. Wu P, Molenaar A, Houben IL (2011) Cement-bound road base materials. Submitted to Delft University of Technology, Delft
43. ASTM (2007) ASTM D5856 standard test method for measurement of hydraulic conductivity of porous material using a rigid-wall, compaction-mold permeameter. American Society for Testing and Materials. Annual Handbook. ASTM International, West Conshohocken, PA
44. Highway AAsS, Officials T (2011) Standard specifications for transportation materials and methods of sampling and testing. American Association of State Highway and Transportation Officials AASHTO, USA
45. de Jesús Arrieta Baldovino J, dos Santos Izzo RL, Rose JL (2021) Effects of freeze–thaw cycles and porosity/cement index on durability, strength and capillary rise of a stabilized silty soil under optimal compaction conditions. *Geotech Geol Eng* 39(1):481–498. <https://doi.org/10.1007/s10706-020-01507-y>
46. Ishikawa T, Lin T, Kawabata S, Kameyama S, Tokoro T (2019) Effect evaluation of freeze-thaw on resilient modulus of unsaturated granular base course material in pavement. *Transportation Geotechnics* 21:100284. <https://doi.org/10.1016/j.trgeo.2019.100284>
47. USBR (2013) DS-13(17)-13: Final: Phase 4. In: Reclamation UBo (ed) Embankment Dams, Chapter 17: Soil-Cement Slope Protection.
48. Diamond S (2004) The microstructure of cement paste and concrete—a visual primer. *Cement Concr Compos* 26(8):919–933. <https://doi.org/10.1016/j.cemconcomp.2004.02.028>
49. Franus W, Panek R, Wdowin M SEM investigation of microstructures in hydration products of portland cement. In: 2nd International multidisciplinary microscopy and microanalysis congress, 2015. Springer, pp 105–112. doi:https://doi.org/10.1007/978-3-319-16919-4_14
50. Scrivener K, Snellings R, Lothenbach B (2018) A practical guide to microstructural analysis of cementitious materials. CRC Press, Cambridge
51. Stark J, Bollmann K (2000) Delayed ettringite formation in concrete. *Nordic Concrete Research-Publications* 23:4–28
52. Stark J, Eckart A, Ludwig H (1997) Influence of C3A content on frost and scaling resistance. *Frost Resistance of Concrete*:100
53. Stark J (1995) The influence of the type of cement on the freeze-thaw / freeze-deicing salt resistance of concrete. *Proc Int Conference Under Severe Cond* 1:245–254
54. Collepardi M (2003) A state-of-the-art review on delayed ettringite attack on concrete. *Cement Concr Compos* 25(4–5):401–407. [https://doi.org/10.1016/S0958-9465\(02\)00080-X](https://doi.org/10.1016/S0958-9465(02)00080-X)
55. Matschei T, Lothenbach B, Glasser F (2007) The AFm phase in Portland cement. *Cem Concr Res* 37(2):118–130. <https://doi.org/10.1016/j.cemconres.2006.10.010>
56. Kirchheim AP, Fernández-Altable V, Monteiro PJM, Dal Molin DCC, Casanova I (2009) Analysis of cubic and orthorhombic C3A hydration in presence of gypsum and lime. *J Mater Sci* 44(8):2038–2045. <https://doi.org/10.1007/s10853-009-3292-3>

Publisher's Note Springer Nature remains neutral with regard to jurisdictional claims in published maps and institutional affiliations.